論文 / 著書情報
Article / Book Information

論題	
Title	Photovoltaic Properties of Si-Based Quantum-Dot-Sensitized Solar Cells Prepared Using Laser Plasma in Liquid
著者	小林 宏輝, P. CHEWCHINDA, 井上 泰徳, 舟窪 浩, 原 亨和, 小田原 修, 和田 裕之
Authors	Hiroki Kobayashi, Pattarin Chewchinda, Yasunori Inoue, Hiroshi Funakubo, Michikazu Hara, Masaie Fujino, Osamu Odawara, Hiroyuki Wada
出典	, vol. 53, num. 1, 010208
Citation	Japanese journal of applied physics, vol. 53, num. 1, 010208
発行日 / Pub. date	2014, 1
DOI	http://dx.doi.org/10.7567/JJAP.53.010208
URL	http://iopscience.iop.org/1347-4065/53/1/010208/
権利情報 / Copyright	本著作物の著作権は（公社）応用物理学会に帰属します。 (c) 2014 The Japan Society of Applied Physics
Note	このファイルは著者（最終）版です。 This file is author (final) version.

doi:10.7567/JJAP.53.010208
Japanese Journal of Applied Physics S53 [1] (2014) 010208

Title:

Photovoltaic Properties of Si-Based Quantum-Dot-Sensitized Solar Cells Prepared using Laser Plasma in Liquid

Authors:

Hiroki Kobayashi[1], Pattarin Chewchinda[1], Yasunori Inoue[2], Hiroshi Funakubo[1], Takeo Yamaguchi[3], Michikazu Hara[2], Masaie Fujino[4], Osamu Odawara[1], Hiroyuki Wada[1]

Affiliation:

1. Interdisciplinary Graduate School of Science and Engineering, Tokyo Institute of Technology, 4259 Nagatsuta, Midori-ku, Yokohama 226-8502 Japan

2. Materials and Structure Laboratory, Tokyo Institute of Technology, 4259 Nagatsuta, Midori-ku, Yokohama 226-8503 Japan

3. Chemical Resources Laboratory, Tokyo Institute of Technology, 4259 Nagatsuta, Midori-ku, Yokohama 226-8503 Japan

4. Chemistry and Materials Science, Gunma National College of Technology, 580 Toba-cho, Maebashi, Gunma 371-8530 Japan

doi:10.7567/JJAP.53.010208
Japanese Journal of Applied Physics S53 [1] (2014) 010208

Corresponding author:

Hiroyuki Wada (Prof. Ph.D.)

E-mail: wada.h.ac@m.titech.ac.jp

Postal address: 4259 Nagatsuta, #J2-41, Midori-ku, Yokohama 226-8502 Japan

Phone/Fax: +81 45 924 5362

doi:10.7567/JJAP.53.010208
Japanese Journal of Applied Physics S53 [1] (2014) 010208

Abstract

Current-voltage characteristics of Si-based quantum-dot-sensitized solar cells (QDSSCs) were investigated. Si nanoparticles were prepared by laser-induced plasma. An Si wafer in ethanol was irradiated with Nd:YAG SHG laser beam. The prepared nanoparticles were identified through X-ray diffraction and Raman spectroscopy. Particle size was measured by a transmission electron microscope (TEM). Highly crystalline Si nanoparticles were observed through TEM. Photoluminescence (PL) spectra of the Si nanoparticles were also measured. Two types of QDSSCs were produced. One included ethanol during the production of TiO_2/Si nanoparticle layer on a transparent conductive oxide electrode because a dispersed Si-nanoparticle ethanol solution was produced using this method; the other type did not involve ethanol. The photovoltaic properties for the former were significantly degraded; the latter maintained good photovoltaic properties. Properties for the latter gradually improved during the measurements. In particular, current density was increased, which increased conversion efficiency. These phenomena are related to changing Si nanoparticle surface conditions.

Keywords: Plasma, Nanoparticle; Laser ablation; Liquid phase

1. Introduction

doi:10.7567/JJAP.53.010208
Japanese Journal of Applied Physics S53 [1] (2014) 010208

Recently, plasma-based processes have been extensively studied due to the unique properties of the devices and materials generated. Plasma is generated using various methods. One unique method includes laser-induced plasma, such as laser ablation, while mainstream plasma generation includes electrical discharge between electrodes. A study on laser ablation in the gas phase was started[1)] after a laser was developed by Townes et al. Laser ablation in liquid was initiated after study using Mossbauer spectroscopy.[2)] Recently, many researchers have studied the generation of nanoparticle of not only metal[3)] but also ceramics.[4,5)] For plasma-based processes, plasma of laser ablation in liquid is confined to a small space,[6)] and Planck's black-body radiation is observed.[7)] Using this method, high temperature and pressure were created in a cavitation bubble, which was desirable for creating novel materials.[8)] Si nanoparticles were prepared using this method.[9,10)]

Recently, dye-sensitized solar cells (DSSCs) have been widely studied.[11)] Quantum-dot-sensitized solar cells (QDSSCs) have also been studied due to their low cost and high conversion efficiency.[12−14)] The QDSSC structure, which is shown in Fig. 1, is similar to DSSC, for which a quantum dot is the sensitizer instead of dye. Electrons are generated in quantum dots, which are semiconductor nanoparticles, through light irradiation and transported to TiO_2 nanoparticles on a transparent conducting oxide

doi:10.7567/JJAP.53.010208
Japanese Journal of Applied Physics S53 [1] (2014) 010208

(TCO) electrode. The counter-electrode is platinum. The gap between the electrodes, which is fixed by spacers, is filled with electrolytes, in which redox reactions occur. The theoretical limitation for QDSSC conversion efficiency is 44 %,[15] although a typical p-n junction silicon solar cell conversion efficiency is 31 % as a result of the low conversion efficiencies at short and long wavelengths.[16] For QDSSCs, multi-exciton generation (MEG) requires a short wavelength, which generates multi-electrons and holes through single-photon irradiation.[12,13,17] For Si nanoparticles, 2.6 excitons were generated using light irradiation at 3.4 eV.[18]

In this study, Si nanoparticles were prepared through laser ablation in liquid, and QDSSCs were successfully produced. Previously some researchers fabricated Si-based QDSSCs[19-26], Si nanoparticles of which were prepared by means other than laser ablation in liquid. Laser ablation in liquid is one of novel methods which create high quality Si nanoparticles. To consider the production process, two types of QDSSCs were compared. To improve the photovoltaic properties, the effect from the measurements was considered.

2. Experimental

Si nanoparticles dispersed in an ethanol solution were prepared through laser

doi:10.7567/JJAP.53.010208
Japanese Journal of Applied Physics S53 [1] (2014) 010208

ablation in liquid. An Si wafer (p type, <100>, 0.6 mm thickness and 11.5-15.5 Ω) in ethanol (42 ml) was irradiated using a pulse Nd:YAG laser (SHG, wavelength: 532 nm, pulse duration: 13 ns, repetition rate: 10 Hz, beam diameter: 14 mm and power: 4.4 W) to produce the Si nanoparticles.

The prepared Si nanoparticles were identified using X ray diffraction (XRD). A solution with dispersed Si nanoparticles was dropped on a single-crystalline MgO substrate and dried. The prepared nanoparticles were also identified though Raman spectroscopy. The prepared solution was dropped on an aluminum pan and dried. The particle size was measured using a transmission electron microscope (TEM). The prepared solution was then dropped on a copper grid and dried overnight at 70 °C in a vacuum. Photoluminescence (PL) spectra of the nanoparticles were measured by a fluorescence spectrophotometer.

QDSSCs were produced using the following procedure. Fluorine-doped tin oxide (FTO, Astellatech Co. transparency: 85%, sheet resistance: 10Ω/□) was used as a TCO electrode given its high thermal stability. Two types of QDSSCs were produced (Si/ethanol and Si). For the Si/ethanol type, the TiO_2 and Si nanoparticle layer was generated using TiO_2 paste (D20-LALT, Solaronix), Si nanoparticles, and ethanol. For the Si type, the layer was generated from TiO_2 paste and Si nanoparticles. The area for

doi:10.7567/JJAP.53.010208
Japanese Journal of Applied Physics S53 [1] (2014) 010208

this layer was 0.237 cm^2, and the thickness was 12 μm; this layer was produced using the squeegee method. Mixed paste was dried at 70 °C for 30 minutes and then it was calcined at 450 °C for 30 minutes in the atmosphere. Indium tin oxide (ITO, Geomatec Co.) with a Pt coating was used as a counter-electrode because of its high conductivity. The gap between FTO and ITO was 17 μm, which was adjusted using the thickness of low-density polyethylene (LDPE) as spacers. The electrolytes included anhydrous acetonitrile, LiI (0.1 M), I_2 (0.05 M), 1,2-dimethyl-3-propylimidazolium iodide (0.6 M), and *tert*-butylpryidine (tBP) (0.5 M). The I-V characteristics were measured at AM1.5 and 100 mW/cm^2 (WACOM, WXS-50S-1.5).

3. Results and discussion

Fig. 2a shows the XRD pattern for nanoparticles on a MgO substrate, which were prepared through laser ablation in liquid. Fig. 2b shows the pattern for the MgO substrate. The data from 40 to 45 degrees were not measured given the strong MgO peak. Fig. 2a indicates that Si nanoparticles were successfully prepared using this method. The inhibition of Si nanoparticle oxidation was also previously reported using ethanol as the solvent.[9,10)] Such inhibition is likely related to ethanol oxidation.

A Raman spectrum is shown in Fig. 3. Although the peak of the bulk silicon

doi:10.7567/JJAP.53.010208
Japanese Journal of Applied Physics S53 [1] (2014) 010208

shown in Fig. 3b was observed at 520 cm^{-1}, that of Si nanoparticle peak shown in Fig. 3a was red-shifted. The particle size can be estimated using the following equation:[27)]

$$\Delta\omega = -\beta\left(\frac{a}{D}\right)^{\gamma} \qquad \text{eq. 1}$$

where $\Delta\omega$ is the Raman frequency shift (cm^{-1}), D is the crystal grain size (nm), a is the lattice parameter (for Si, 0.543 nm), and β and γ are parameters that describe vibrational confinement (for the Richter model, β=52.3 cm^{-1} and γ=1.586). The estimated particle size from several measurements was 4.1±2.5 nm. Full width at half maximum (FWHM) of Si nanoparticles and Si wafer were 5.3 and 3.3 cm^{-1}, respectively. The slight broadening of the peak would be due to the particle size distribution of Si nanoparticles.

The TEM images for the prepared nanoparticles are shown in Fig. 4. The Si and TiO_2 mixture was used to produce QDSSCs. Fig. 4a-c (low and high magnification) only indicates Si nanoparticles. Fig. 4d-f shows a mixture of Si and TiO_2 nanoparticles. The lattice fringe, which indicated that highly crystalline Si nanoparticles were obtained by this method, was observed in the high magnification images. The parallelogram-like crystals in Fig. 4d-f are TiO_2. Si nanoparticle adherence to the TiO_2 crystal is shown in Fig. 4f. The particle size distribution for Si nanoparticles is shown in Fig. 5. This size approximately corresponds to the average particle size measured using Raman spectroscopy. The particle size distribution is slightly larger. However, it

doi:10.7567/JJAP.53.010208
Japanese Journal of Applied Physics S53 [1] (2014) 010208

would vary Si bandgap related to quantum confinement[28,29] and then would lead to absorption of various wavelength light, which would result in high conversion efficiency. Mechanism of formation of Si nanoparticle by laser ablation in liquid is still controversial. One of considerable ones would be the followings.[8] Target is heated by laser beam and then cavitation bubble is formed. Nanoparticles would be created in the bubble. Particle size would be related to lifetime of the bubble, which was a few hundred microseconds, because nanoparticle grew in the bubble.

Fig. 6 shows PL spectrum of Si nanoparticles. The bandgap of bulk Si is approximately 1.1 eV, which means the absorption-edge is 1.1 μm. In contrast, the peak emission wavelength in Fig. 6 was blue-shifted. The reason of emission of Si nanoparticle is still controversial. This blue shift would be related to quantum confinement by nanosizing Si particle.

In this study, two types of QDSSCs were generated, Si/ethanol and Si. To produce the transparent electrode for the Si/ethanol type, dispersed Si nanoparticles in an ethanol solution and TiO_2 paste were mixed. To generate the Si type, Si nanoparticle powder and TiO_2 paste were mixed, which included only Si and TiO_2. To understand the effect from ethanol, three types of QDSSCs were generated, and the photovoltaic properties were measured, as shown in Fig. 7. The short-circuit current density (J_{SC}),

doi:10.7567/JJAP.53.010208
Japanese Journal of Applied Physics S53 [1] (2014) 010208

open-circuit voltage (V_{OC}), fill factor (*FF*) and energy conversion efficiency (η) are shown in Table 1. Current-voltage characteristic of QDSSC, transparent electrode of which included TiO_2 and ethanol, was significantly degraded in comparison with that of only TiO_2. When only Si nanoparticles were added to the transparent electrode, these properties were improved up to those of only TiO_2. Ethanol interfusion had a significantly negative effect on the QDSSCs. Therefore, the Si-type QDSSC, which did not include ethanol, was successfully generated. Fig. 8 shows the current-voltage characteristics for the QDSSCs one day after they were generated to fill the TiO_2 and Si nanoparticle gaps with electrolytes. The J_{SC}, V_{OC}, *FF* and η are shown in Table 2. In this case, the samples were not degraded, and the energy conversion efficiency for the QDSSC with Si nanoparticles and TiO_2 was 17 times greater than for only TiO_2 as a result of the enhanced photovoltaic parameter values. Because most research on QDSSCs is related to Cd compounds, Si-based QDSSCs are not often reported, and the energy conversion efficiency for Si-based QDSSCs is not high. However, Si-based QDSSC research is important because Si is a nontoxic, stable and widely used material. The photovoltaic properties in this study are comparable to those in previous studies.[19-26] The electrolyte of recent Si-based QDSSC was polysulfide.[21-26] In this case, high value of J_{SC} is obtained although V_{OC} and *FF* are low. The comparatively

doi:10.7567/JJAP.53.010208
Japanese Journal of Applied Physics S53 [1] (2014) 010208

high stability would be related to non-reactivity to Si. In contrast, iodide electrolyte is possible to achieve high V_{OC} and *FF*. The increase in J_{SC} in this study would be related to the reaction between Si and iodide electrolyte. The researches on various parameters which are including electrolyte are important to increase conversion efficiency of Si-based QDSSC because this research is less common.

Fig. 9 indicates the photovoltaic properties for this QDSSC as a function of the number of measurements. The total time for the measurements was 8.5 hours. J_{SC} significantly increased with an increase in the number of measurements, which increased η, but V_{OC} and *FF* were approximately constant. Without photovoltaic property measurements, the parameters for this QDSSC, such as J_{SC}, did not increase. Typically, half an hour after generation, the photovoltaic properties are improved for DSSCs because electrolytes diffuse into the gaps between the TiO_2 particles.[30] The saturation time for this phenomenon depends on the electrode, dye and cell structure. However, there may be other reasons for this QDSSC because a longer time was required for the J_{SC} to increase to the saturated value. In general, an increase in J_{SC} and decreases in V_{OC}, *FF* and η are observed with increasing cell temperatures for DSSCs.[30] The values for this QDSSC did not change when they were not measured. Therefore, our results are not attributed to the cell temperature and are related to the optical

doi:10.7567/JJAP.53.010208
Japanese Journal of Applied Physics S53 [1] (2014) 010208

irradiation and electricity generation. The simple equivalent circuit for solar cell is shown in Fig. 10.[31,32] I_L is constant-current source. A diode represents the electrical properties of the pn-junction. R_s is a series resistance. R_{sh} is shunt resistance. R_L is load resistance connected to solar cell. The relationship between *FF* and series resistance (R_s) is defined in the following equations:[32]

$$FF = FF_0\left(1 - \frac{R_s}{R_{ch}}\right), \qquad \text{eq. 2}$$

$$R_{ch} = \frac{V_{mp}}{I_{mp}}, \qquad \text{eq. 3}$$

where FF_0 is the maximum fill factor, R_{ch} is the characteristic resistance of a solar cell, V_{mp} is the voltage at maximum power, and I_{mp} is the current at maximum power. Fig. 11 shows R_{ch} as a function of time. Because the *FF* of this QDSSC was constant (Fig. 9c), FF_0 should be constant. Therefore, R_s should decrease because R_{ch} gradually decreased. The decrease in R_s produces an increase in J_{SC}. Typically, R_s is the sum of the TCO sheet resistance, the TCO and TiO_2 contact resistance, the resistance related to charge-transfer processes at the Pt counter-electrodes, the resistance related to electron transfer at the TiO_2/quantum dot/electrolyte interface and the resistance related to carrier transport through ions in the electrolyte. For this QDSSC, the factor influenced should be the resistance related to electron transfer at the TiO_2/quantum dot/electrolyte interface. R_s is reduced for two possible reasons. One is the reduction reaction at the

doi:10.7567/JJAP.53.010208
Japanese Journal of Applied Physics S53 [1] (2014) 010208

native silicon dioxide layer on the Si nanoparticle, which would prevent electron transfer at the interface. The other is that photocorrosion dissolves the native silicon dioxide layer on the Si nanoparticle. These effects should increase J_{SC}.

4. Conclusion

Silicon nanoparticles were successfully prepared using laser ablation in liquid. Certain particles indicated lattice fringe, which implies high crystallinity. The particle size was approximately 5 nm, which was observed using TEM. In this study, Si nanoparticles dispersed in ethanol were generated. We generated two types of QDSSCs. One included ethanol, and the other did not. Ethanol degraded the photovoltaic properties. The properties obtained in this study, such as V_{OC} (0.49 V), were comparably higher than for previous Si-based QDSSCs. The J_{SC} and energy conversion efficiency gradually increased during the photovoltaic measurements.

5. Acknowledgements

We would like to thank Prof. K. Nakamura (laser ablation), Ms. H. Tokimori (TEM) and Mr. Y. Suzuki (XRD) in Tokyo Tech. This work was supported by the Materials and Structure Laboratory (Tokyo Tech. collaborative research) and JSPS

doi:10.7567/JJAP.53.010208
Japanese Journal of Applied Physics S53 [1] (2014) 010208

KAKENHI Grant Number 23119506.

6. References

1) F. Brech and L. Cross : Appl. Spectroscopy **16** (1962) 59.

2) P. P. Patil, D. M. Phase, S. A. Kulkarni, S. V. Ghaisas, S. K. Kulkarni, S. M. Kanetkar and S. B. Ogale: Phys. Rev. Lett. **58** (1987) 3.

3）F. Mafune, J. Y. Kohno, Y. Takeda, T. Kondow and H. Sawabe, J. Phys. Chem. B, **104** (2000) 8333.

4） H. Usui, Y. Shimizu, T. Sasaki and N. Koshizaki: J Phys. Chem. B, **109** (2005) 120.

5) C. L. Sajti, R. Sattari, B. N. Chichkov and S. Barcikowski: J. Phys. Chem. C, **114** (2010) 2421.

6) N. Takada, T. Nakano and K. Sasaki: Appl. Surf. Sci. **255** (2009) 9572.

7) K. Sasaki and N. Takada: Pure Appl. Chem. **82** (2010) 1317.

8) W. Soliman, T. Nakano, N. Takada and K. Sasaki: Jpn. J. Appl. Phys. **49** (2010) 116202.

9) S. Yang, W. Cai, H. Zhang, X. Xu and H. Zeng: J. Phys. Chem. C, **113** (2009) 19091.

10) K. Abderrafi, R. G. Calzada, M. B. Gongalsky, I. Suarez, R. Abarques, V. S. Chirvony, V. Y. Timoshenko, R. Ibanez and J. P. Martinez-Pastor: J. Phys. Chem. C,

doi:10.7567/JJAP.53.010208
Japanese Journal of Applied Physics S53 [1] (2014) 010208

115 (2011) 5147.

11) B. O'Regan, M. Gratzel, Nature **353** (1991) 737.

12) A. J. Nozik: Physica E, **14** (2002) 115.

13) P. V. Kamat: J. Phys. Chem. C, **112** (2008) 18737.

14) L. J. Diguna, Q. Shen, J. Kobayashi and T. Toyoda: Appl. Phys. Lett. **91** (2007) 023116.

15) A. J. Nozik: Chem. Phys. Lett. **457** (2008) 3.

16) W. Shockley and H.J. Queisser, J. Appl. Phys. **32** (1961) 510.

17) V. I. Klimov: J. Phys. Chem. B, **110** (2006) 16827.

18) M. C. Beard, K. P. Knutsen, P. Yu, J. M. Luther, Q. Song, W. K. Metzger, R. J. Ellingson and A. J. Nozik: Nano Lett. **7** (2007) 2506.

19) V. Švrček, I. Turkevych, K. Hara and M. Kondo: Nanotechnol. 21 (2010) 215203.

20) Y. Kawashima, K. Nakahara, H. Sato, G. Uchida, K. Koga, M. Shiratani and M. Kondo: Trans. Mater. Res. Soc. Jpn. 35 (2010) 597.

21) G. Uchida, K. Yamamoto, M. Sato, Y. Kawashima, K. Nakahara, K. Kamataki, N. Itagaki, K. Koga and M. Shiratani, Jpn. J. Appl. Phys. 51 (2012) 01AD01.

22) H. Seo, Y. Wang, G. Uchida, K. Kamataki, N. Itagaki, K. Koga and M. Shiratani, Electrochimica Acta, 87 (2013) 213.

doi:10.7567/JJAP.53.010208
Japanese Journal of Applied Physics S53 [1] (2014) 010208

23) H. Seo, Y. Wang, G. Uchida, K. Kamataki, N. Itagaki, K. Koga and M. Shiratani, Electrochimica Acta, 95 (2013) 43.

24) H. Seo, Y. Wang, M. Sato, G. Uchida, K. Kamataki, N. Itagaki, K. Koga, M. Shiratani: Jpn. J. Appl. Phys. 52 (2013) 01AD05.

25) G. Uchida, M. Sato, H. Seo, K. Kamataki, N. Itagaki, K. Koga and M. Shiratani: Thin Solid Films (2013) in print.

26) H. Seo, Y. Wang, M. Sato, G. Uchida, K. Koga, N. Itagaki, K. Kamataki and M. Shiratani: Thin Solid Films (2013) in print.

27) G. Faraci, S. Gibilisco, P. Russo, A. R. Pennisi and S. L. Rosa: Phys. Rev. B, **73** (2006) 033307.

28) Al. L. Efros, A. L. Efros, Sov. Phys. Semicond. **16** (1982) 772.

29) L. E. Brus J. Chem. Phys. **80** (1984) 4403.

30) K. Hara, S. Igari, S. Takano and G. Fujihashi: Electrochem. **73** (2005) 887.

31) S. M. Sze: *Semiconductor devices Physics and technology* (John Wiley & Sons, New York, 2002) Chap. 9.

32) N. Koide, A. Islam, Y. Chiba and L. Han: J. Photochem. Photobio. A: Chem. **182** (2006) 296.

doi:10.7567/JJAP.53.010208
Japanese Journal of Applied Physics S53 [1] (2014) 010208

Figure captions

Fig. 1. Schematic of SDSSC.

Fig. 2. XRD patterns for samples prepared using laser ablation in liquid. a) nanoparticles and MgO substrate, b) MgO substrate.

Fig. 3. Raman spectra of a) Sample prepared through laser ablation in liquid and b) Si wafer. Inset: Enlargement of peaks.

Fig. 4. TEM images for a sample prepared using laser ablation in liquid.

Fig. 5. Particle size distribution of a sample prepared through laser ablation in liquid.

Fig. 6. PL spectrum of a sample prepared through laser ablation in liquid.

Fig. 7. Current–voltage characteristics for the Si-based QDSSC used to investigate the effect from ethanol.

Fig. 8. Current–voltage characteristics for the Si-based QDSSC.

Fig. 9. Photovoltaic properties for this QDSSC as a function of the number of measurements. (a: V_{OC}, b: J_{SC}, c: FF and d: η)

Fig. 10. Schematic of equivalent circuit of solar cell.

Fig. 11. R_{ch} as a function of time.

Table 1. QDSSC photovoltaic properties used to investigate the effect from ethanol.

doi:10.7567/JJAP.53.010208
Japanese Journal of Applied Physics S53 [1] (2014) 010208

Table 2. QDSSC photovoltaic properties.

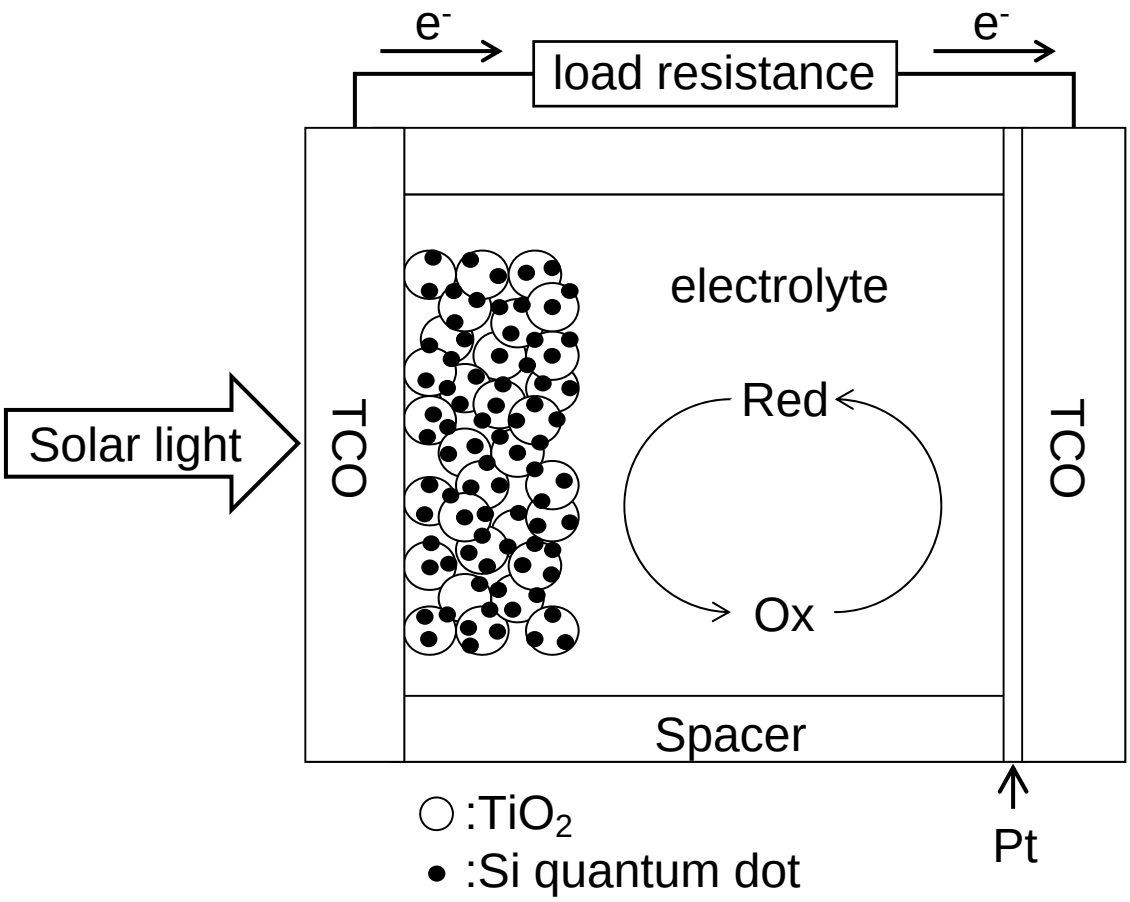

Fig. 1. Schematic of SDSSC.

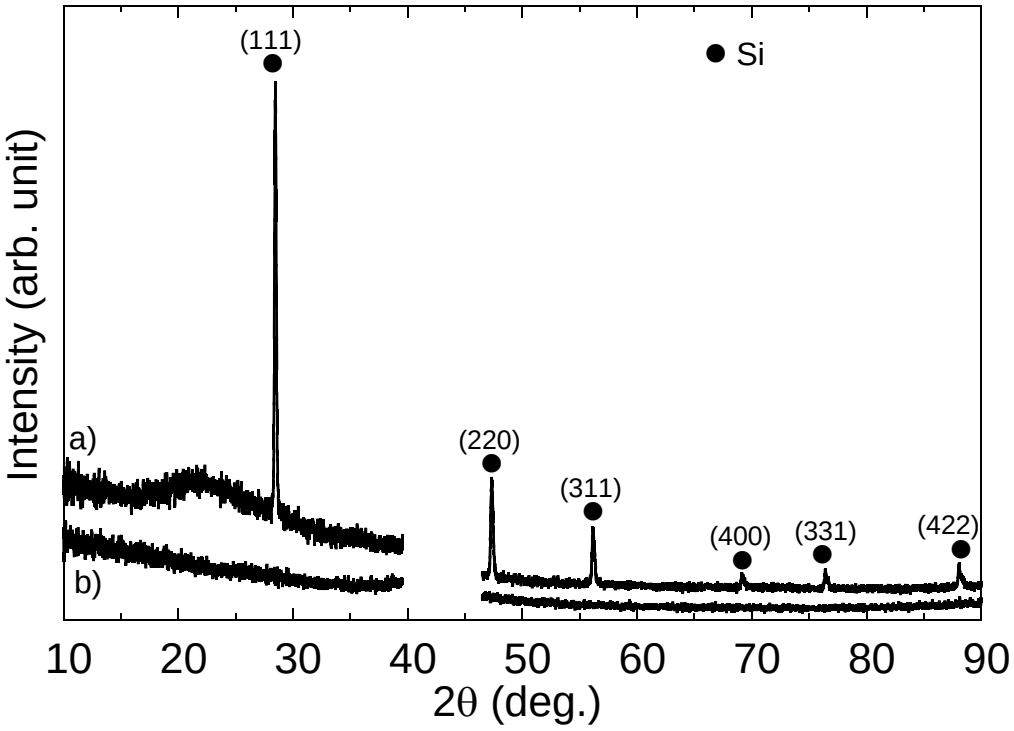

Fig. 2. XRD patterns for samples prepared using laser ablation in liquid. a) nanoparticles and MgO substrate, b) MgO substrate.

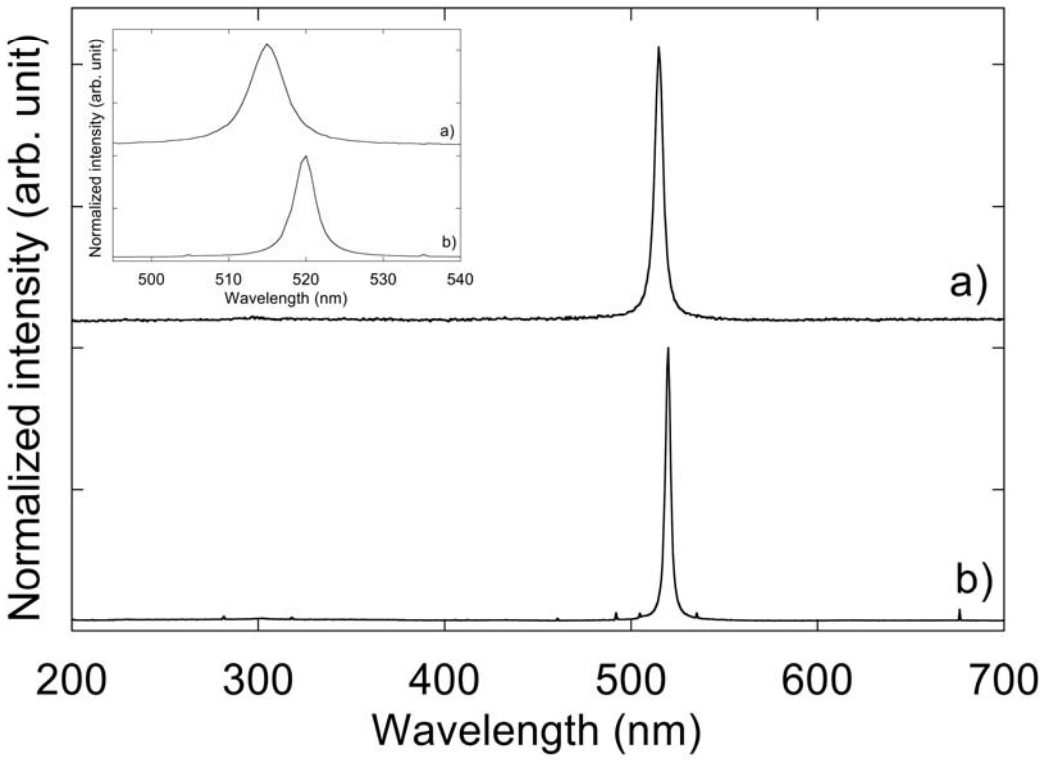

Fig. 3. Raman spectra of a) Sample prepared through laser ablation in liquid and b) Si wafer. Inset: Enlargement of peaks.

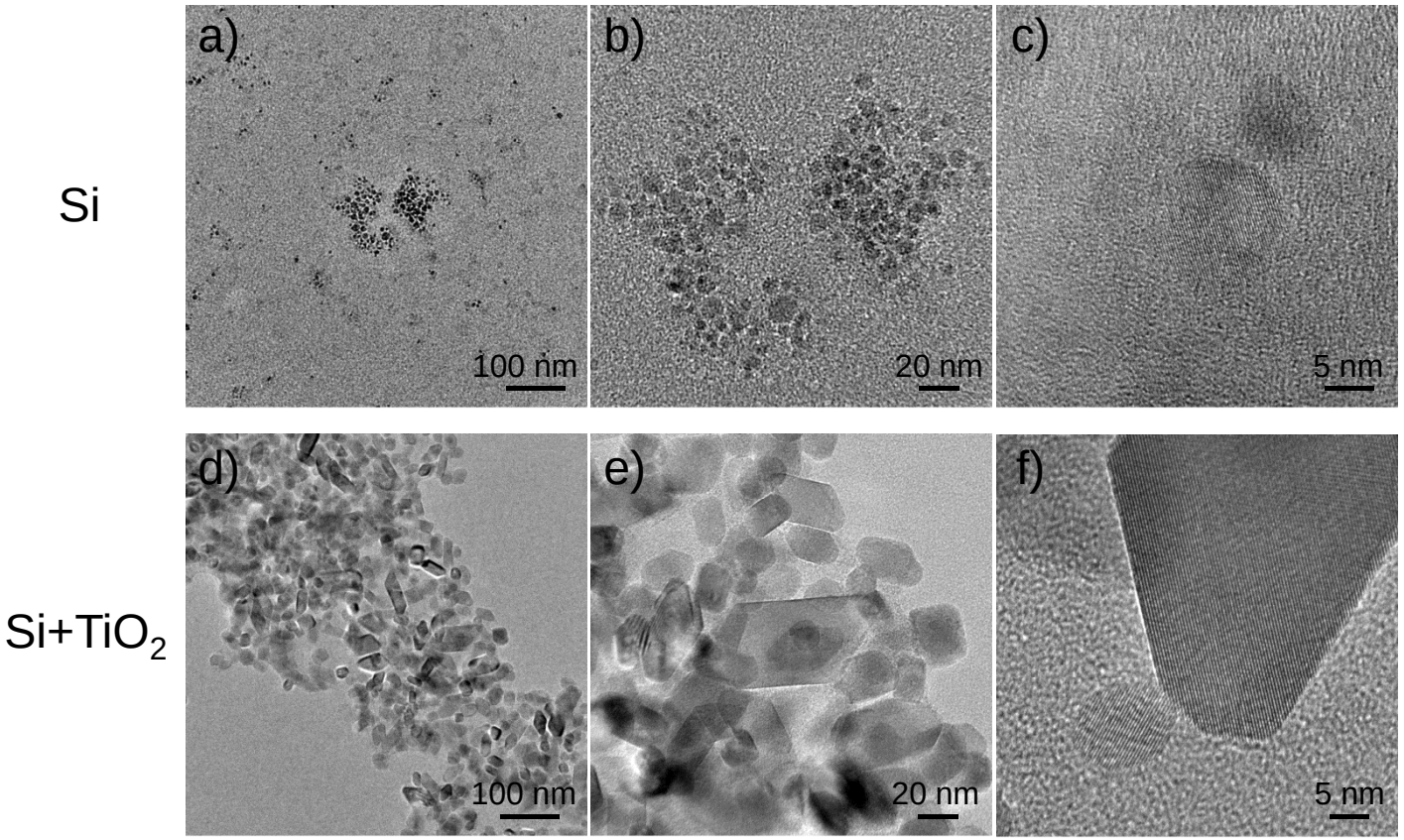

Fig. 4. TEM images for a sample prepared using laser ablation in liquid.

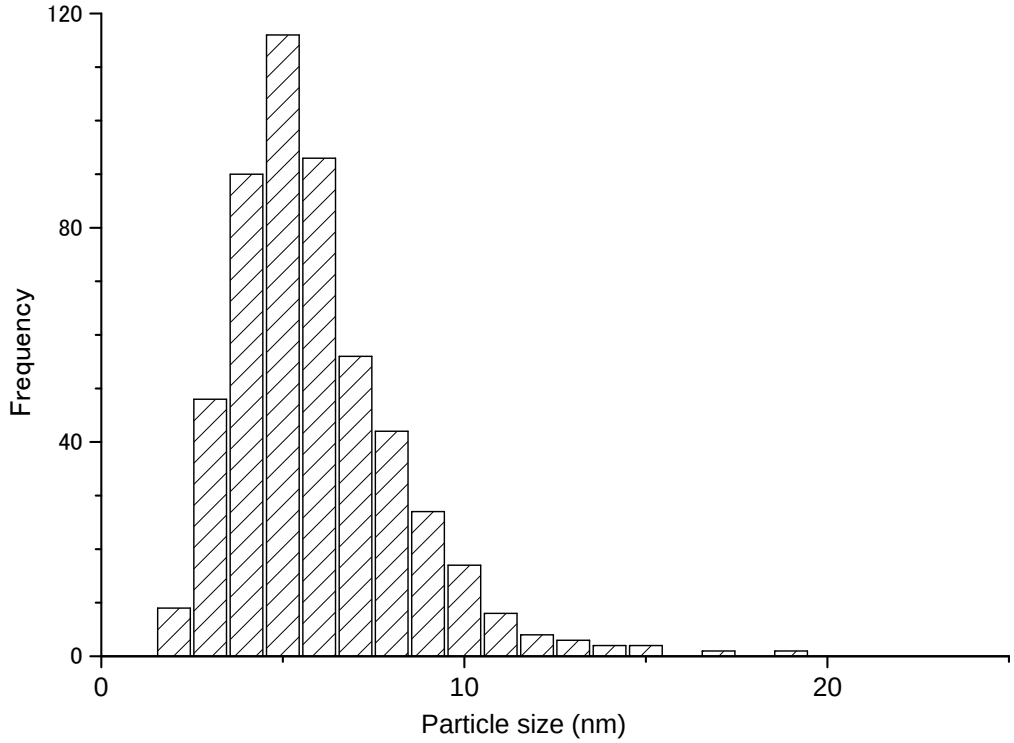

Fig. 5. Particle size distribution of a sample prepared through laser ablation in liquid.

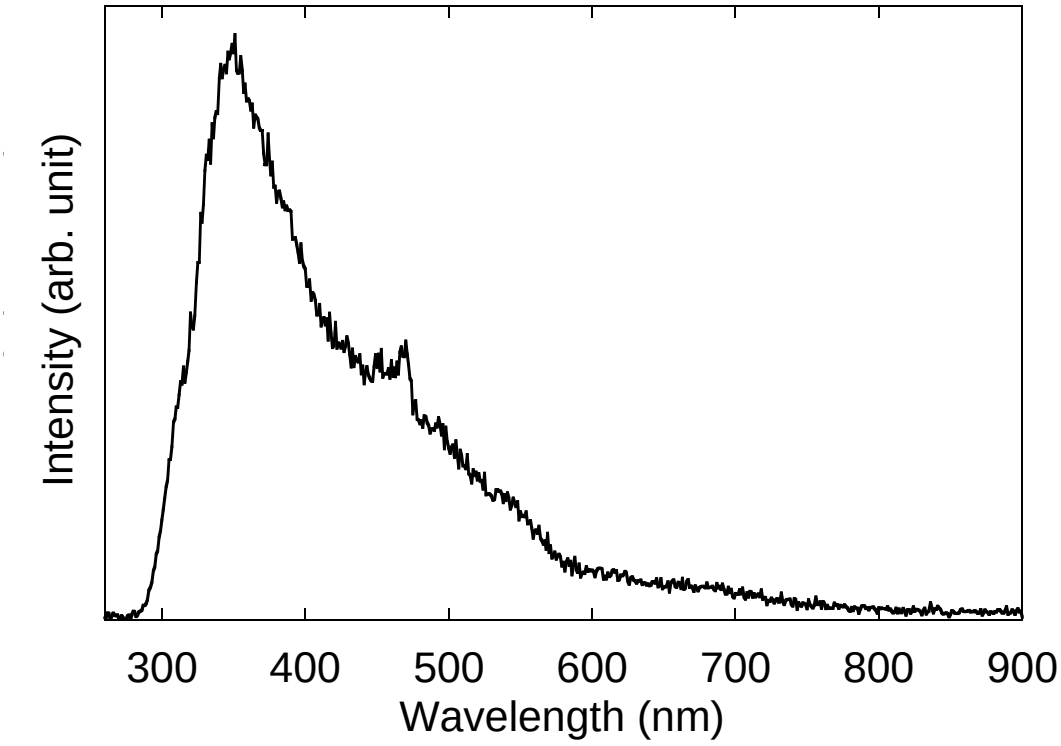

Fig. 6. PL spectrum of a sample prepared through laser ablation in liquid.

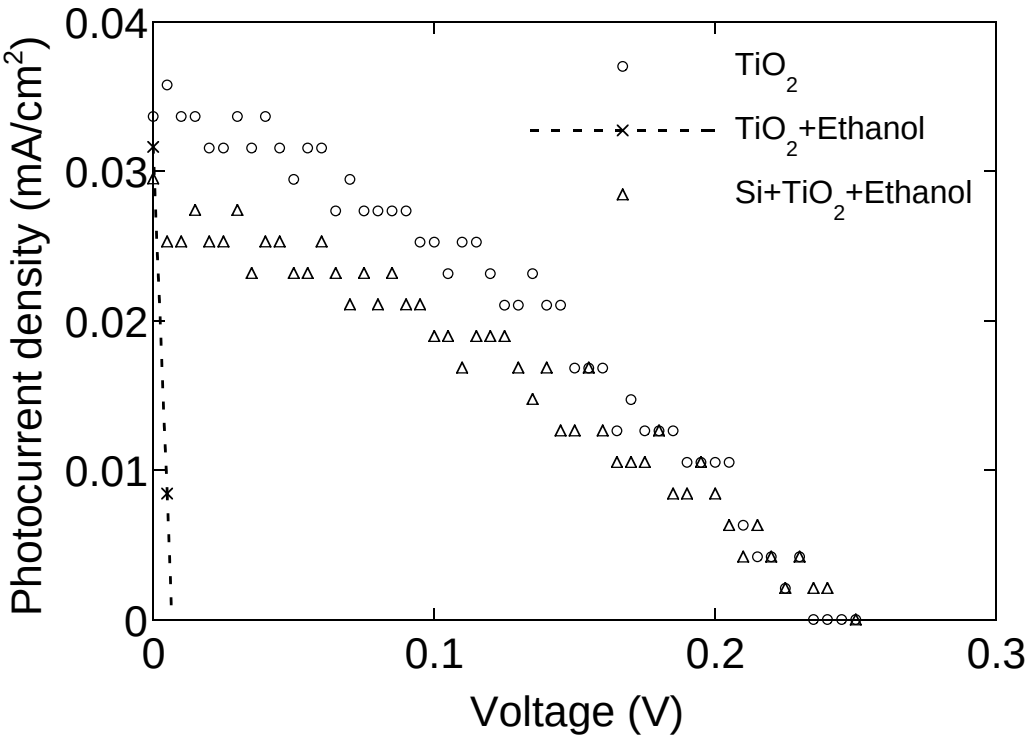

Fig. 7. Current -voltage characteristics for the Si-based QDSSC used to investigate the effect from ethanol.

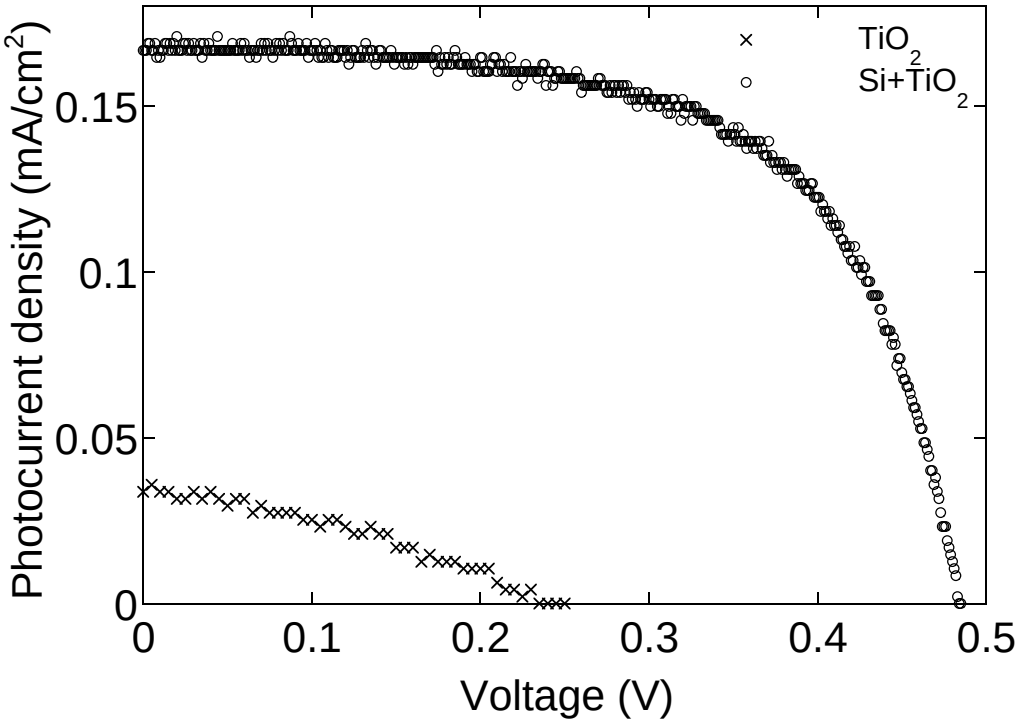

Fig. 8. Current -voltage characteristics for the Si-based QDSSC.

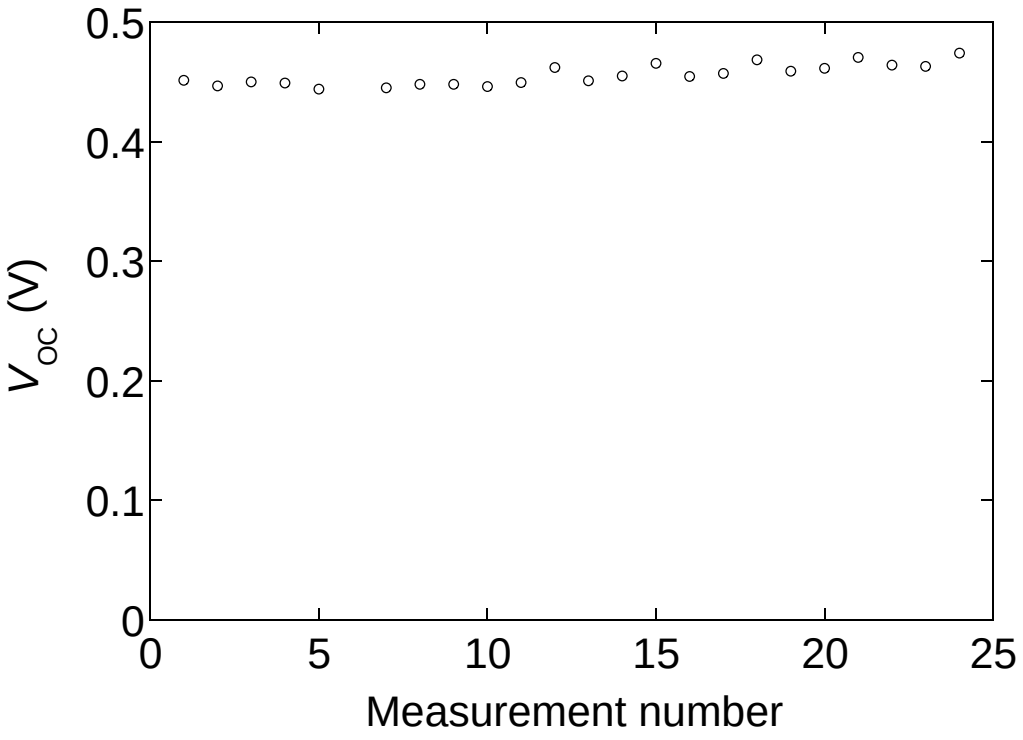

Fig. 9a. Photovoltaic properties for this QDSSC as a function of the number of measurements. (V_{OC})

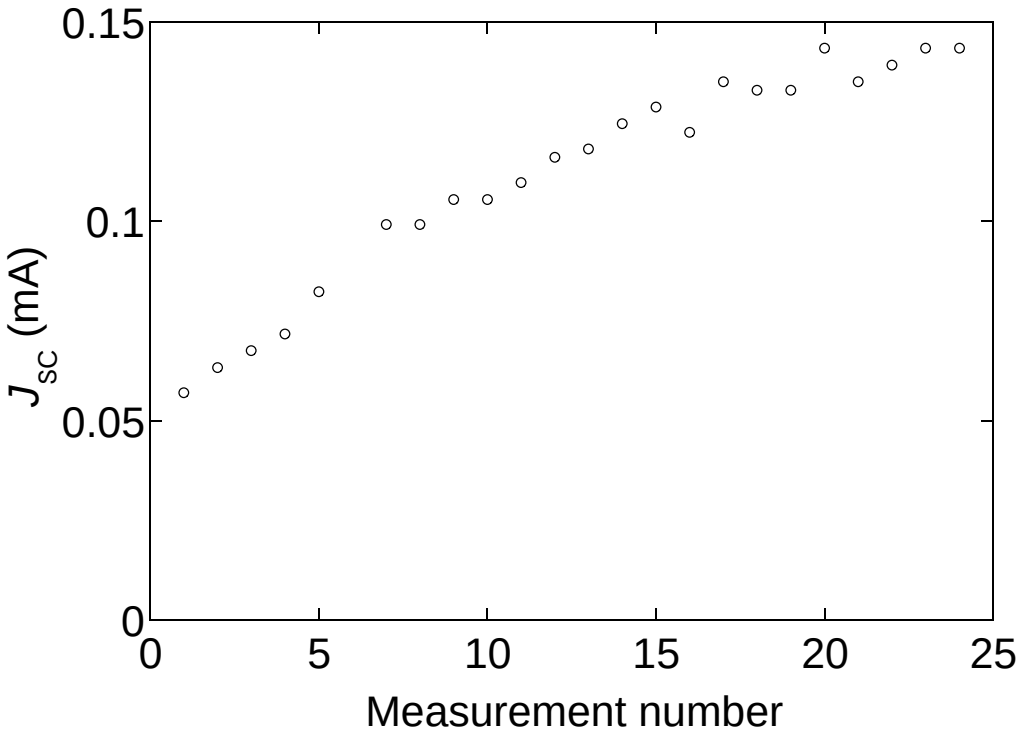

Fig. 9b. Photovoltaic properties for this QDSSC as a function of the number of measurements. (J_{SC})

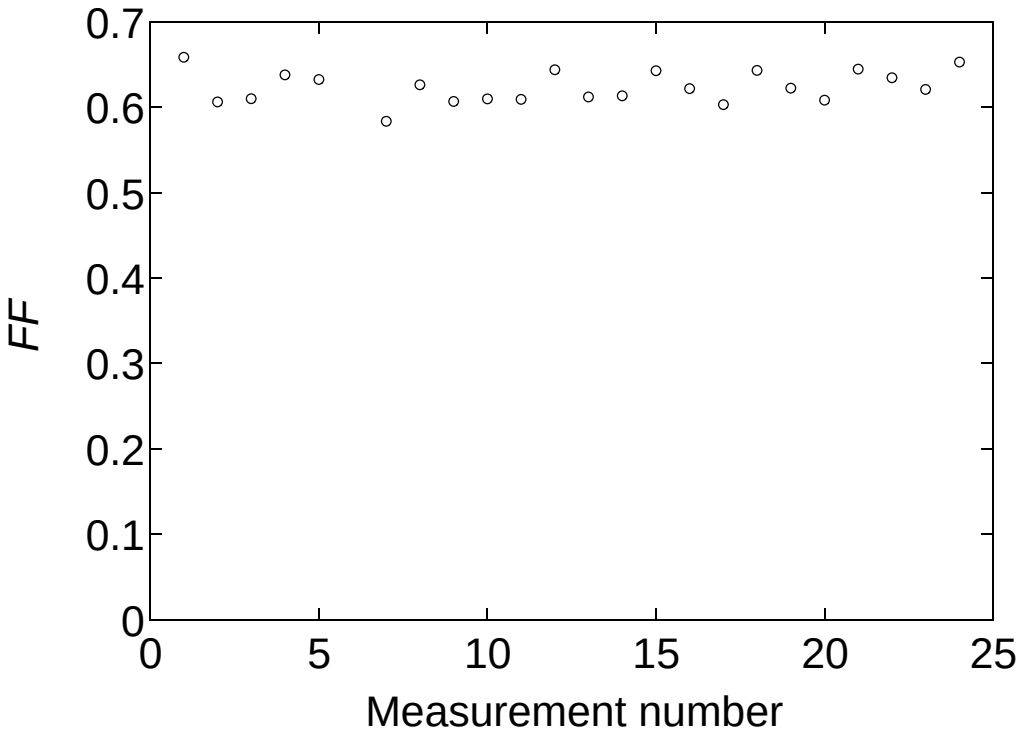

Fig. 9c. Photovoltaic properties for this QDSSC as a function of the number of measurements.
(*FF*)

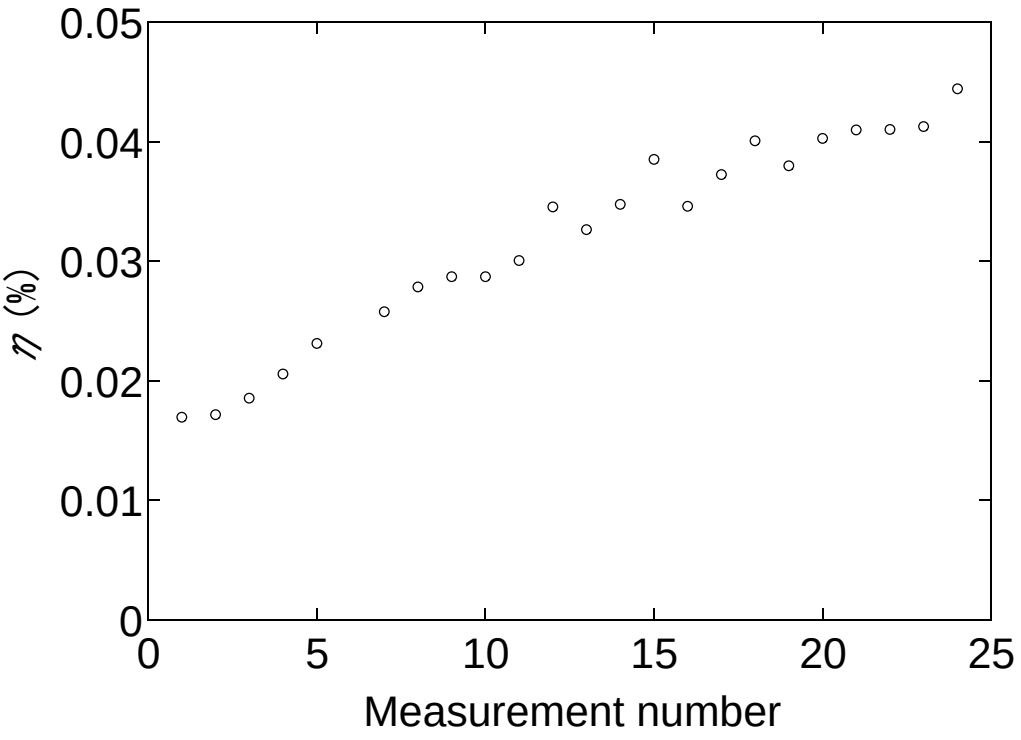

Fig. 9d. Photovoltaic properties for this QDSSC as a function of the number of measurements.
(η)

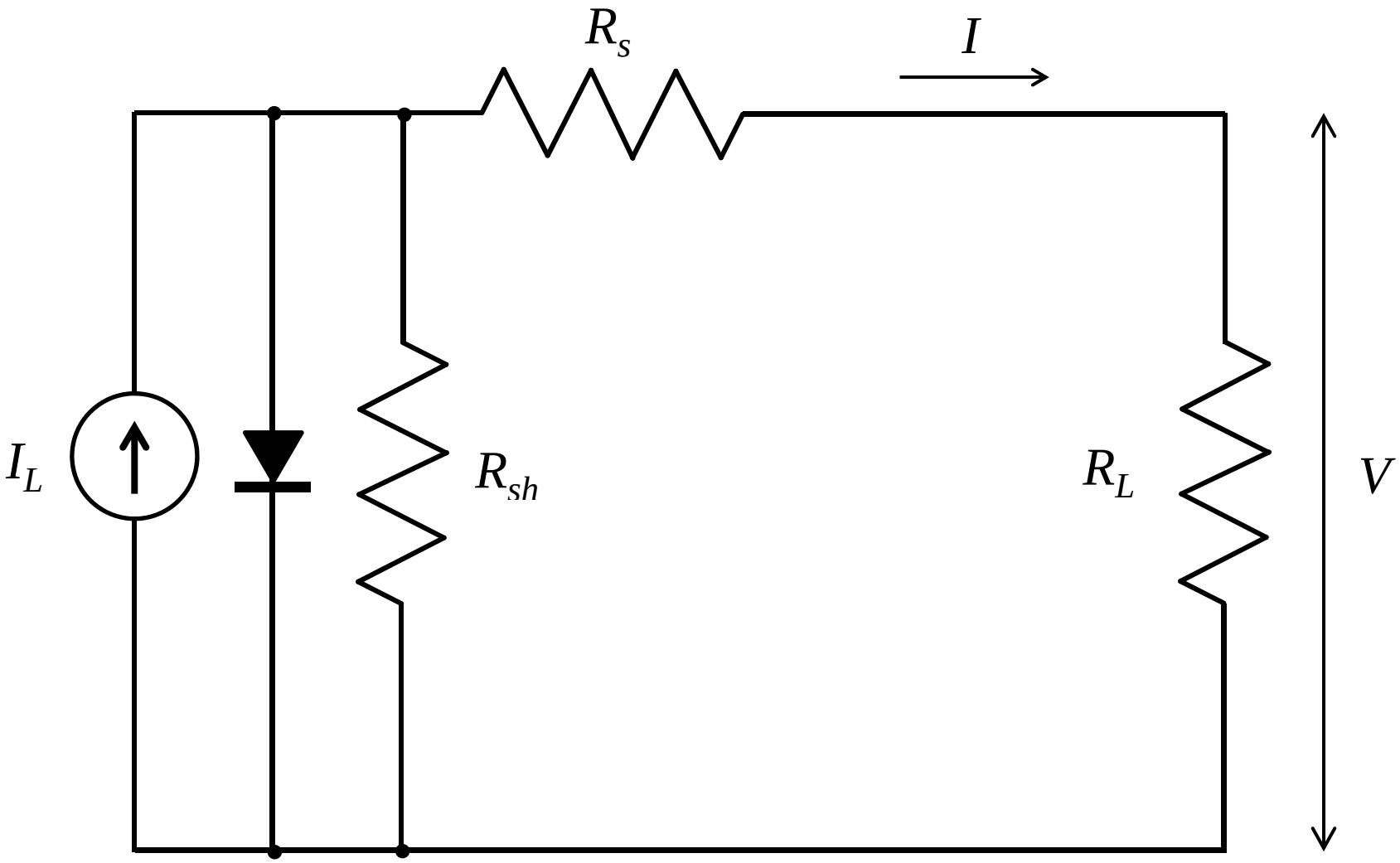

Fig. 10. Schematic of equivalent circuit of solar cell.

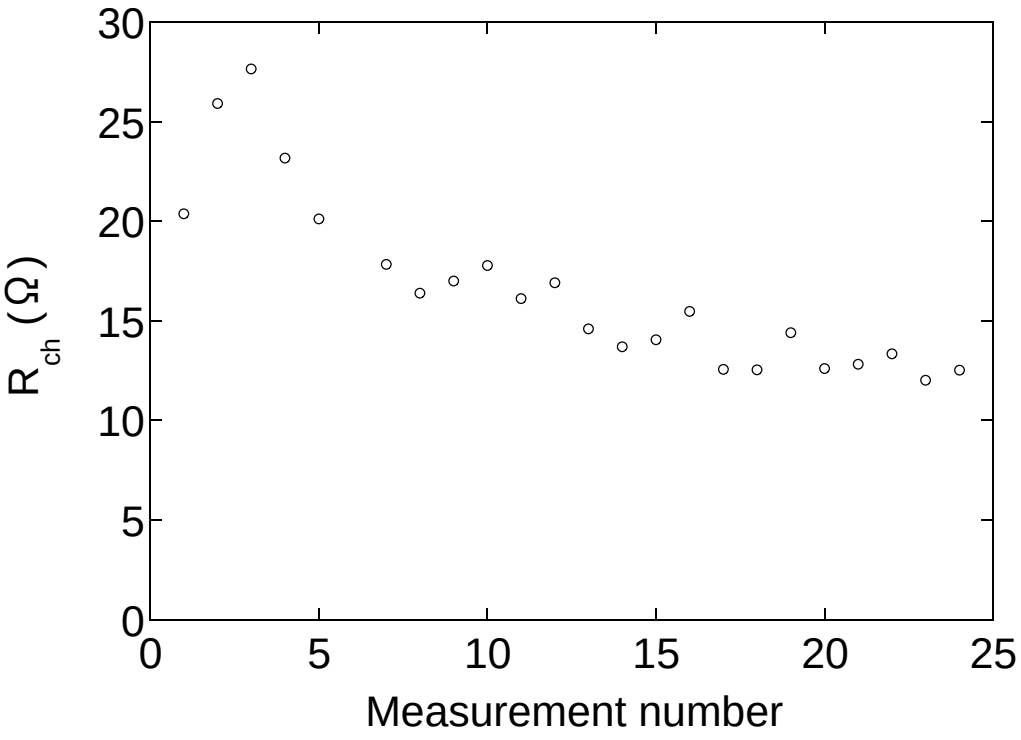

Fig. 11. R_{ch} as a function of time.

Table 1. QDSSC photovoltaic properties used to investigate the effect from ethanol.

	TiO_2	TiO_2 + Ethanol	Si + TiO_2 + Ethanol
J_{SC} (mA/cm^2)	0.034	0.032	0.030
V_{OC} (V)	0.25	0.0067	0.25
FF	0.37	0.27	0.35
η (%)	0.0031	0.000056	0.0026

Table 2. QDSSC photovoltaic properties.

	TiO_2	Si + TiO_2
J_{SC} (mA/cm^2)	0.034	0.17
V_{OC} (V)	0.25	0.49
FF	0.37	0.64
η (%)	0.0031	0.052